npj | Climate and Atmospheric Science

www.nature.com/npjclimatsci

ARTICLE OPEN

Check for updates

Beyond megacities: tracking air pollution from urban areas and biomass burning in Brazil

Rafaela Squizzato[1,3]✉, Thiago Nogueira[1,3], Leila D. Martins[2], Jorge A. Martins[2], Rosana Astolfo[1], Carolyne Bueno Machado[1], Maria de Fatima Andrade[1] and Edmilson Dias de Freitas[1]✉

Most of the world's population lives in rural areas or small to medium-sized cities (totalling 68% of the world population), all of which are impacted by distant air pollution sources. In Brazil, primary pollutant emissions have decreased in urban centres because of government actions, while secondary pollutants such as surface ozone (O_3) increased. In addition, O_3 and its precursors can be worsening air quality in areas already affected by biofuels production, especially ethanol. We provide almost 3 months of hourly data (June 7, 2019 to August 25, 2019) for concentrations of O_3, CO_2 and other priority pollutants from a mobile station positioned to distinguish among pollutant plumes (biomass burning, metropolitan area of São Paulo (MASP) and other cities). Although the concentrations of O_3 and CO_2 were highest in the plumes from biomass burning, the MASP accounted for up to 80% of the O_3 concentration in communities over 200 km away.

npj Climate and Atmospheric Science (2021)4:17 ; https://doi.org/10.1038/s41612-021-00173-y

INTRODUCTION

High surface ozone (O_3) concentrations pose a serious concern for modern societies because they have been associated with deleterious effects on human health[1,2], damage to crops[3,4] and climate change[5,6]. Reversing the impacts of anthropogenic air pollution demands actions aimed at reducing dependency on fossil fuel in the transport, industry and energy sectors[7,8]. As a result of attempts to reduce that dependency, limit emissions of greenhouse gases and lower ambient concentrations of atmospheric pollutants, the global consumption of biofuels, such as ethanol, has doubled in the last two decades[9].

By 2019, the participation of ethanol (hydrated and anhydrous) in the matrix of fuels used by Otto cycle engines (in passenger cars and other light-duty vehicles) in Brazil reached 48.3%[10]. Brazil is the second largest ethanol producer in the world[11], and the state of São Paulo accounts for 55% of the sugarcane production in the country[12], sugarcane occupying 70% of the land devoted to agriculture in the state (Fig. 1).

In the past, controlled burning of sugarcane fields was responsible for considerable emissions of gases and particles; government actions have limited that practice, leading to lower air pollutant emissions in the state[13]. However, the material known as bagasse (sugarcane leaves/sheaths) is used as fuel in electric power plants, which are sources of atmospheric pollutants[14,15], generating emissions throughout the year. Paradoxically, the rural regions of the state play an important role in improving air quality in the large urban centres by providing cleaner fuels. Rural areas may be affected by pollution from biofuel production, as well as receiving air pollutants by regional transport from urban centres. Unfortunately, without sufficient air pollutant monitoring data, the important role that the transition from fossil fuel to biofuels can play in mitigating the impacts on climate and health cannot be fully understood. One limitation of previous studies is the paucity of data for rural areas, which hinders the evaluation of the distribution of air pollutants, especially O_3, on a regional scale.

O_3 is a short-lived climate pollutant (SLCP), with an atmospheric lifetime of ~23 days[16], hence it can be transported to other regions. The most important contributors to anthropogenic climate change, after CO_2, are methane, hydrofluorocarbon, black carbon and O_3[17]. Although several recent studies have addressed O_3 concentrations at sites within the fourth largest megacity in the world—the metropolitan area of São Paulo (MASP)[18]—and in urban areas of the state of São Paulo[19–26], none performed an in-depth analysis of the regional effects that emissions from the MASP and the transport of gases from biomass burning have on O_3 concentrations. Long-range transport of O_3 is seen in other parts of the world. For example, Doherty[27] and Lin et al.[28] showed the intercontinental transport of O_3 from East Asia to western North America and the flow of O_3-rich air from Eurasia toward Hawaii, based on long-term measurements performed at Mauna Loa observatory. There is also evidence that regional O_3 (averaged over large areas extending well beyond cities) is increasing at some locations, particularly in densely populated areas, as pointed out by Madronich et al.[29] who found a 6–7% increase per decade in the Indo-Gangetic Plains, as well as in Beijing during the 2008 Summer Olympics. In Brazil, Boian and Andrade[30] using the Caltech–Carnegie Mellon 3-D Eulerian photochemical model (CIT) showed the transport of O_3 from the MASP to the city of Campinas, 90 km to the northwest. The surface measurements showed a second peak of O_3 that the modelling showed to be due to the transport of O_3 and O_3 precursors from the MASP to that location.

In recent years, air pollutant emissions from thermal power plants have increased because of greater demand, bagasse-fired power plants generating ~25% of the energy produced in the state of São Paulo[31]. Nationwide, such plants emit up to 27 Tg of CO_2 annually, slightly higher than that estimated for the plants burning fossil fuels[14]. However, despite climate concerns, CO_2 is rarely measured at air quality monitoring stations.

[1]Departamento de Ciências Atmosféricas, Instituto de Astronomia, Geofísica e Ciências Atmosféricas, Universidade de São Paulo, São Paulo, Brazil. [2]Federal University of Technology—Paraná, Londrina, PR, Brazil. [3]These authors contributed equally: Rafaela Squizzato, Thiago Nogueira. ✉email: rafaela.squizzato@iag.usp.br; edmilson.freitas@iag.usp.br

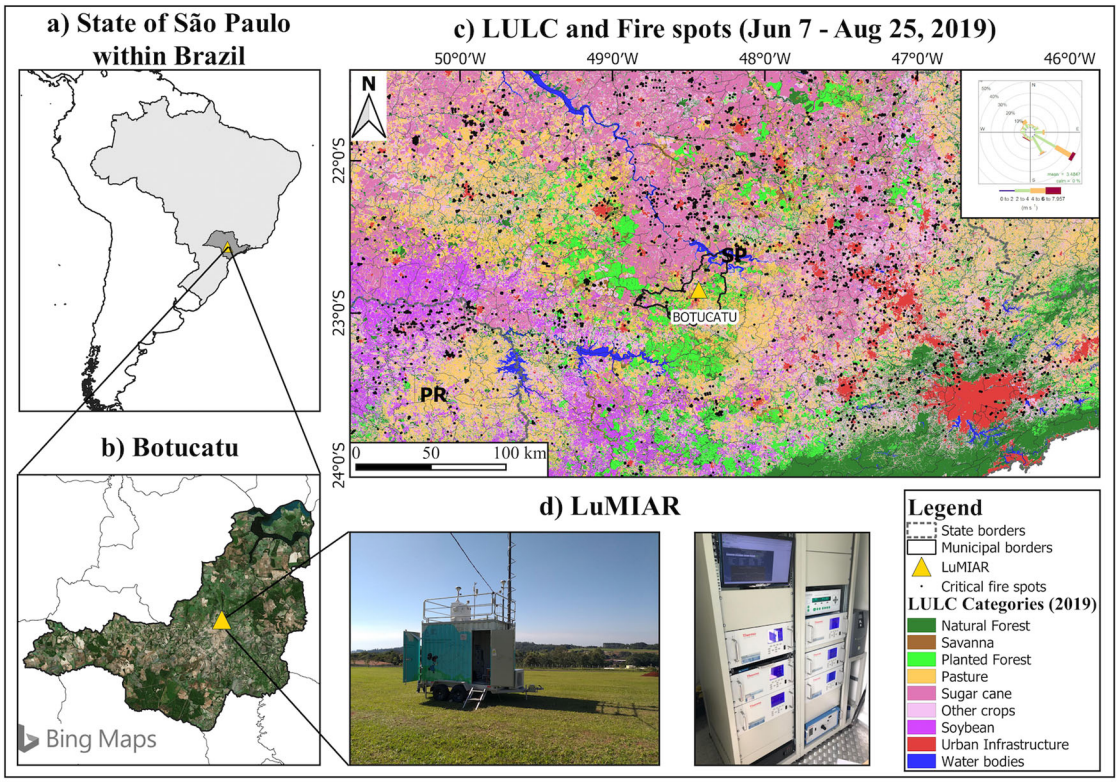

Fig. 1 Location and characterization of the study area. a, **b** Maps showing the location of the sampling site (within the city of Botucatu, Brazil). **c** Land use and land cover (LULC) for the study area and its surroundings in 2019. PR: (state of) Paraná; SP: (state of) São Paulo. **d** External and internal view of the laboratório móvel para pesquisa e monitoramento da qualidade do ar (LuMIAR, mobile laboratory for air quality monitoring and research) used in this study. Source: The LULC map was obtained after the reclassification of MapBiomas data (Project MapBiomas—Collection 5 of Brazilian Land Cover and Use Map Series, accessed on December 2, 2020, through the link: https://mapbiomas.org/colecoes-mapbiomas-1?cama_set_language=pt-BR)[56], a public mapping of Brazil, based on Landsat images with a spatial resolution of 30 m. Fire spots were provided by INPE, Instituto Nacional de Pesquisas Espaciais, 2020, Portal de Monitoramento de Queimadas e Incêndios Florestais. Available at http://www.inpe.br/queimadas. Accessed on December 14, 2020.

The objective of this study was to assess priority pollutants (NO_2, SO_2, CO and O_3), together with CO_2, at a strategic geographical position (Fig. 1), discriminating the pollutant plumes from urban areas and from biomass burning in the state of São Paulo, with an emphasis on O_3. We performed an in-depth analysis of the roles that pollutant sources in the MASP and biomass burning (mainly of sugarcane by-products such as bagasse and field residue) play in the behaviour of O_3 in the state, using the city of Botucatu, which has 150,000 inhabitants, as an example. We chose Botucatu because it is representative of the type of area in which the majority of the population of Brazil lives.

RESULTS

Overview

Samples were collected continuously over a total of 80 days (56 weekdays and 24 weekend days, from June 7 to August 25, 2019), with a 1-h resolution for all pollutants. Of the 80 days sampled, none of the pollutants exceeded the limit recommended in the national air quality standards (NAQS) established in Brazilian National Environmental Council Resolution no. 491/2018[32]. However, O_3 often (on 21 days) surpassed the concentration limit recommended by the World Health Organization (8-h mean of 51 ppbv/100 μg m^{-3}), which is more restrictive than is that recommended in the Brazilian NAQS (8-h mean of 71 ppbv/140 μg m^{-3}). On some days, O_3 concentrations exceeded that limit. The pattern of pollutant concentrations as well as daily cycle and meteorological parameters are detailed in the Supplementary Results and illustrated in Supplementary Figs 1–4. The results of a quantile regression of the influence of meteorological conditions and primary pollutants on O_3 concentrations are shown in Supplementary Fig. 5, demonstrating that regional transport is the main driver of the elevated O_3 concentrations observed.

Circulation and regional transport

Polar annulus plots[33] discriminate the effect of regional transport, showing the hourly changes in O_3 concentrations and the effects of wind direction. Figure 2a shows that O_3 concentrations were highest in plumes from the northwest and northeast, with significant contributions also from the southeast. The O_3 concentrations from the northwest tended to remain high until the end of the day. The nearest medium-sized city (Botucatu) appears not to be an important source of air pollution, as suggested by our finding that winds from the south and southwest did not contribute to high O_3 concentrations. Those trends are consistent with the conditional probability function (CPF) plots and bivariate polar plots[33] shown in Fig. 2b, c. The CPF plots indicate the probability of a selected concentration from each wind direction, whereas the bivariate polar plots use a generalised additive model to interpolate between averaged data points for wind direction and speed. The results also indicate that O_3 concentrations were generally higher when air parcels from the northwest arrived at higher speeds (≥5 m s^{-1}). The regions to the northwest and northeast of the study site are categorised as agricultural areas. During the study period, those regions showed high fire potential (Fig. 1). In addition, winds from the northwest and northeast can be associated with O_3 transport from the northern and central-west regions of Brazil, where the

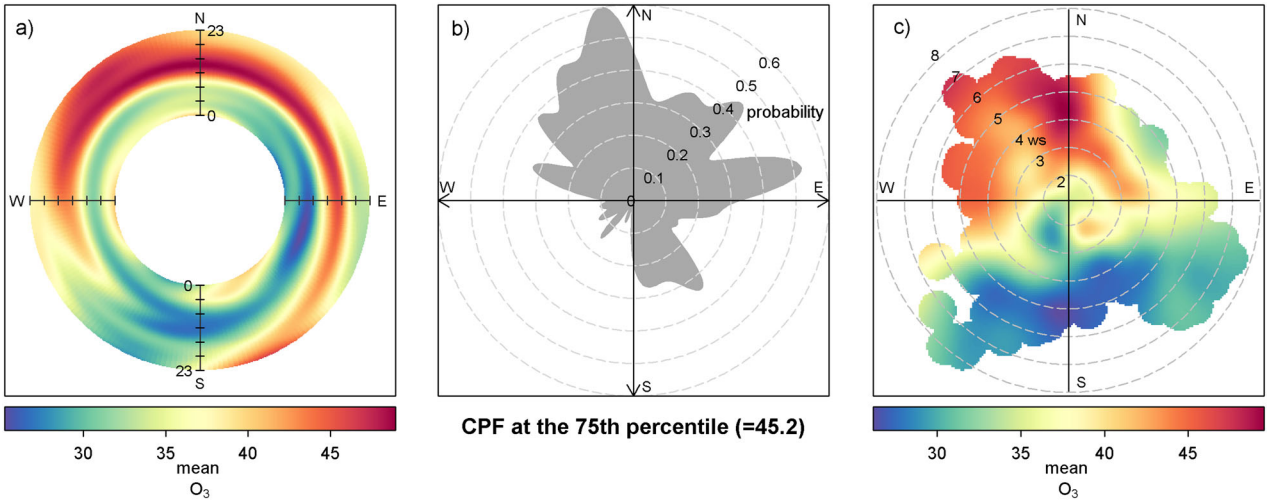

Fig. 2 Identifying potential sources of increased ozone (O_3) concentrations at the sampling site. a Polar annulus plot depicting the mean hourly O_3 concentrations for the entire study period. **b** Conditional probability function (CPF) plot of O_3 concentrations above the 75th percentile (45.2 ppbv). **c** Bivariate polar plot of O_3 concentrations.

intensity of biomass burning is high, mainly in September (the end of the dry season), when most air masses move toward the south. The impact of frontal systems on the biomass burning smoke plume is described in the Supplementary Results, as is that of long-distance transport on O_3 concentrations. As shown in Supplementary Fig. 6, the number of registered fire spots increased over the study period. Supplementary Figures 7–9 show that O_3 and CO concentrations were highest when the wind came from the northwest and northeast direction, which does not happen to NO_x (see more details in Supplementary Results). The fact that, at the Botucatu station, NO_x did not respond to the increase in the number of fire foci shows that NO_x reacted before reaching the sampling site.

To elucidate the contribution from each region, we generated CPF plots for the quartile ranges of O_3 concentrations during the daytime (8:00 a.m.–6:59 p.m. LT, Supplementary Fig. 10) and nighttime (7:00 p.m.–7:59 a.m. LT, Supplementary Fig. 11). Daytime O_3 in the first quartile arrived on winds from the southeast (predominantly from the MASP) and at higher speeds (≥6 m s^{-1}), whereas fourth-quartile daytime O_3 was more likely to arrive on winds from the northwest. Nighttime O_3 in the first quartile most often arrived on winds from the southwest (predominantly from Botucatu). The second-quartile nighttime O_3 showed high probability (≤0.9) of being near the upper limit when the winds were from the southeast, which supports our hypothesis that the high mean nighttime O_3 concentration (39.5 ± 11.1 ppbv) was due to regional transport from the MASP. Together with the low concentrations of NO, the O_3 concentrations remain high overnight due to the absence of O_3 titration ($NO + O_3 = NO_2 + O_2$). Although there is NO_3 formation ($NO_2 + O_3 = NO_3 + O_2$) at night, it is not enough to decrease the O_3 concentrations significantly[34,35]. At ranges above the second quartile, nighttime contributions from the city of Botucatu were observed, as was a local nighttime contribution from the sampling site.

Figure 3 shows a scatter plot of the $O_3 + NO_2$ (O_x) and $NO + NO_2$ (NO_x) values, together with the linear regression line for the correlation between the two. The overall mean contribution of regional transport to O_3 concentrations at the sampling site, obtained by determining the intercept from the linear equation, was 32 ppbv. However, that contribution depends on the wind direction (Supplementary Fig. 12). The greatest mean contribution (43 ppbv) was from the northwest. The mean contribution from the southeast (i.e. the MASP) was 30 ppbv and was attributed to regional transport.

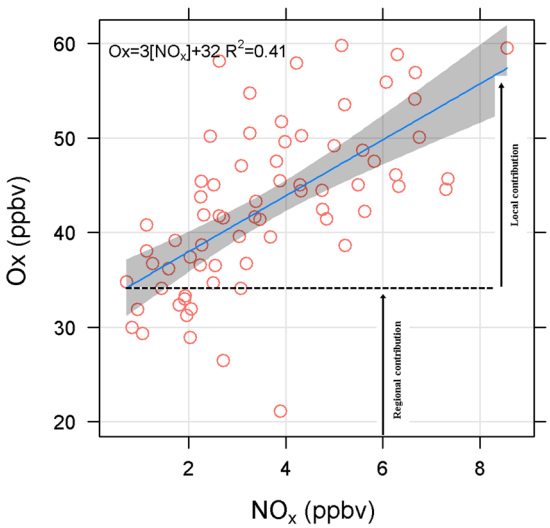

Fig. 3 Ozone (O_3) contribution to regional transport. The figure shows the correlation between the daylight mean mixing ratio for $O_3 + NO_2$ (O_x) and that for $NO + NO_2$ (NO_x). The blue line was obtained by linear regression analysis, and the grey shaded area indicates the confidence interval. The intercept gives the contribution of O_3 to regional transport, whereas the slope gives the contribution of primary pollutants[55]. The model is based on sampling performed from 8:00 a.m. to 6:00 p.m. LT daily.

Figure 4 shows the average daily concentration of O_3, together with the proportional contribution of each wind sectors on each day. We can see that winds from the southeast were predominant during the study period (as can also be seen in Supplementary Fig. 3), those winds resulting in significantly higher average daily concentrations (~36 ppbv, Supplementary Table 1). Although winds from the northwest were less common, the mean for that wind sector (42.5 ppbv) was higher than the 35.8 ppbv observed for the southeast sector (Supplementary Table 1). Given that the prevailing wind is from the southeast (see the Supplementary Results), that the long-range transport from that sector was 30 ppbv (Supplementary Fig. 12) and that the mean concentration for the whole period was 37.2 ppbv, we estimated that ≈80% of O_3 concentration at the sampling site was due to its transport from the MASP.

Using CO_2/CO correlation to track regional transport of O_3

Figure 5 shows the linear regression of the relationship between CO_2 and CO (ppmv ppmv^{-1}), which can be interpreted as a proxy for CO_2 emissions. Higher slope values for the CO_2/CO correlations were found when the winds were from the northwest, north and northeast (44, 46 and 53, respectively). High CO_2 emissions were also identified when the winds were from the east and west, with slope values for the CO_2/CO correlation of 45 and 49, respectively. Those high CO_2 emissions are related to biomass burning (Fig. 1), including the burning of bagasse in thermal power plants. Conversely, when the winds were from the southwest and south (i.e. from the urban area of Botucatu), the slope values were lower (29 and 39, respectively). Even when the wind was from the southeast, the slope value was only 37, indicating that CO_2 emissions from the MASP had a minimal impact at the sampling site. We also found that higher CO_2 emissions were accompanied by a higher mean O_3 concentration (~42 ppbv) when the wind was from the northeast/northwest, whereas lower CO_2 emissions were accompanied by a lower mean O_3 concentration (~35 ppbv) when the wind was from the southeast/southwest.

Comparing the sampling site with other sites in São Paulo

Supplementary Figure 13 shows the diel cycle for O_3 obtained at the sampling site (Botucatu) in comparison with those obtained at other air quality monitoring stations operated by the Sao Paulo State Companhia Ambiental do Estado de São Paulo (CETESB, Environmental Protection Agency), some (Piracicaba, Bauru and Tatuí) located near the Botucatu site and others (Ibirapuera and Pico do Jaraguá) located in the MASP. During the night (12:00 a.m.–5:00 a.m. LT), O_3 concentrations at the Botucatu station were up to 72, 85 and 59% higher than those recorded at the Bauru, Piracicaba and Tatuí stations, respectively, as well as being higher than those recorded at the background sites in the MASP—up to 74 and 34% higher at the urban (Ibirapuera) and sub-urban (Pico do Jaraguá) stations, respectively. During the most photochemically active hours (12:00 p.m.–5:00 p.m. LT), O_3 concentrations were 21 and 32% higher at the sampling site than at the Piracicaba and Tatuí sites.

Supplementary Figure 14 shows the diel cycle for NO_x (NO_2 + NO) concentrations. During the period of greatest emission of these compounds (between 8:00 a.m. and 6:00 p.m. LT) at the Bauru, Ibirapuera and Piracicaba stations, the concentrations were, respectively, up to 61.8, 82.7 and 66.1% higher than those recorded at Botucatu. Those concentrations were 47.9% higher at the Pico do Jaraguá station than at Botucatu.

In addition, we compared O_3 and NO_x concentrations on weekdays and weekends at the Botucatu, Ibirapuera and Pico do Jaraguá sites (Supplementary Fig. 15). Although NO_x showed a significant reduction on weekends at all sites (nonparametric Mann–Whitney U test, $p < 0.05$), O_3 performed differently. At the Botucatu and Pico do Jaraguá sites, the O_3 concentration showed no significant change ($p > 0.05$) on weekends during the most photochemically active hours (12:00 p.m.–5:00 p.m. LT), although an increase in O_3 concentration was observed at the Ibirapuera station ($p < 0.05$).

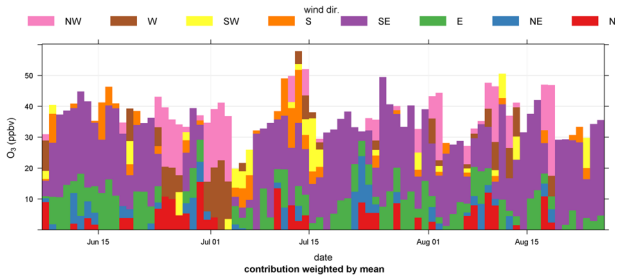

Fig. 4 O_3 time series plot categorised into wind sectors. Daily variation in O_3 concentrations by proportional contributions of wind sectors (north, northeast, east, southeast, south, southwest, west and northwest). The O_3 concentrations are represented as stacked bars to show the proportional contribution of each wind sector.

DISCUSSION

Although government policies have reduced air pollution in urban areas of Brazil[20], there is a paucity of data on air quality outside urban areas. The results obtained here help elucidate the impact of ethanol production activities on O_3 concentrations in rural areas. These findings are particularly timely as several countries now consider implementing their intended nationally determined contributions (NDCs) to reduce fossil fuel emissions, as stipulated in the 2015 Paris Agreement on climate change, by increasing biofuel use. It is therefore worthwhile to consider the local and distant impacts that biofuel production/use have on air quality. Taken together, our data on pollutant concentrations, CO_2 emissions and their relationships with meteorological parameters illustrate that sources in small cities have less impact on air quality in remote areas than do those in megacities and agricultural activities/biomass burning. Understanding O_3 behaviour in rural areas is an urgent topic because, when combined with significant

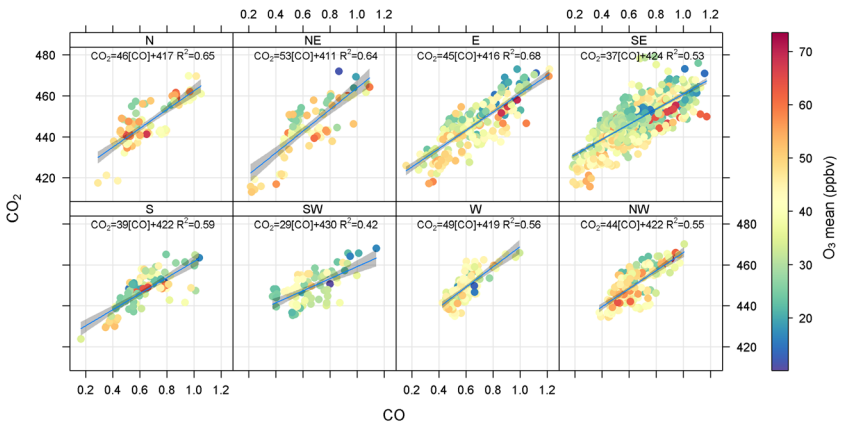

Fig. 5 Estimated CO_2 emissions and their relationship to ozone (O_3) concentrations. Scatter plots showing how the relationship between CO_2 and CO affected O_3 concentrations (colour-coded by intensity) in each wind quadrant. The slope obtained from the linear regression can be interpreted as a proxy for CO_2 emissions, lower slope values indicating lower CO_2 emissions (usually from low-efficiency combustion processes, such as burning biomass in the open field) and higher values indicating higher CO_2 emissions (from combustion processes that are more efficient, such as the burning of sugarcane bagasse to generate electricity).

measures to cut CO_2 emissions, reducing SLCP concentrations plays an important role in slowing the rate of global warming and achieving the Paris Agreement goal of limiting it to 2 °C.

Our finding that O_3 concentrations were higher at the sampling site than at the Pico do Jaraguá site is quite interesting because the latter is in an ideal position within the MASP to track pollutant transport on a regional scale. That underscores the fact that the air quality in the region is affected not only by activities in the MASP but also by local activities. It is noteworthy that ~8% of the 15.6 million litres of ethanol produced in the state is consumed in the MASP[10,36]. The use of ethanol as fuel advances in vehicle engine technology and changes in public policy have arguably been responsible for the recent improvement in air quality in the MASP[20]. However, although the use of ethanol results in a reduction in regulated compounds (NO_x and CO) and CO_2, an increase in the consumption of this biofuel can generate an increase in O_3 concentrations. That is because incomplete combustion of ethanol results in higher emissions of carbonyl compounds, mainly acetaldehyde and other VOCs[37–41], for which the reactivity to produce O_3 in the atmosphere is at least 4.3 times higher than that for ethanol[42].

O_3 concentration did not increase over the weekend at Botucatu, which indicates that the atmospheric regime is not the same as in the central area of the MASP (Ibirapuera station). The increase in O_3 concentration on weekends is a well-known phenomenon and is associated with a VOC-limited atmospheric regime in urban areas[39], where a reduction in NO_x concentrations on weekends results in an increase in O_3 concentration. This phenomenon has already been documented for the MASP[25,43]. However, in rural areas or places with high NO_x emissions, where a reduction in NO_x concentration during weekends results in a decrease in O_3 concentration, an NO_x-limited atmospheric regime is expected. Nevertheless, we observed that the concentration did not decrease on weekends, which supports our hypothesis that O_3 is predominantly transported from other areas and not formed locally. Therefore, O_3 concentrations are often higher in such places than in neighbouring cities, as well as being higher than in the MASP. In addition, due to the low NO concentration locally, these concentrations remain higher for longer.

The CO_2 emissions observed at our sampling site were higher than those reported for other rural areas around the world. At a rural site near Beijing, China, the CO_2/CO correlation was reported to be 13.3–21.2 (ppmv ppmv^{-1})[44]. Nevertheless, the CO_2/CO correlation obtained in the present study was lower than those reported for urban areas of the USA, such as Pasadena, California[45] and Cookeville, Tennessee[46], where it was ~87 and ~104 (ppmv ppmv^{-1}), respectively, albeit higher than the 22 (ppmv ppmv^{-1}) reported for urban areas of India where other biofuels are burned (mainly during the winter)[47].

Understanding and reducing the number of O_3 episodes caused by regional transport are relevant for improving crop yields. By 2050, global warming could reduce crop production by more than 10%, and O_3 trends could either exacerbate or offset a substantial fraction of climate impacts, underscoring the importance of air quality management in agricultural planning[4]. Studies evaluating NDCs and scenarios limiting global warming to 2 °C have shown that O_3 reductions would increase production of O_3-sensitive crops, including sugarcane and soybeans[6].

One limitation of our study is the lack of information on the concentrations of VOCs, which should be explored in future studies. The monitoring site seems to reflect an NO_x-limited regime, which is common in rural areas, as evidenced by the fact that the reduction in NO_x concentrations on weekends did not cause an increase in O_3 concentrations (Supplementary Fig. 15). Another characteristic of an NO_x-limited atmosphere is that it is less dependent on changes in VOC concentrations. This effect was evidenced in a study carried out in the city of Araraquara (200 km from our sampling site), where a significant increase in ethene concentrations in emissions related to the sugarcane industry was not found to result in a significant increase in O_3 concentrations at the surface[48].

METHODS

Sampling site

The sampling site in the current study was located in the south-central region of the state of São Paulo (22.85 S; 48.43 W, 200 km from the MASP), far from any city centre, and there were no physical barriers around the site. The MASP is the largest urban agglomeration in South America, with more than 21 million inhabitants and a vehicular fleet up to 8 million, and accounts for 82% of the gross domestic product of the state[49]. The areas to the north, northeast and northwest of the sampling site are dedicated to agriculture, especially sugarcane cultivation. There are ethanol refineries and bagasse-fired thermal power plants throughout the northern area of the state. The closest municipality (Botucatu), located to the south/southwest of the site, is a small city, like hundreds of others in the state of São Paulo, with a population of 148.130 inhabitants[50]. Figure 1 shows the position of the site, together with the land use and land cover classifications in the state.

Data collection and analysis

We employed a mobile laboratory with a complete suite of equipment to evaluate air quality by measuring concentrations of gaseous pollutants and CO_2. Details about instrumentation and calibration are included in the Supplementary Methods. Sampling occurred continuously throughout the winter of 2019 (from June 7 to August 25). The data management and statistical analyses were performed with the openair package[33] of the R statistical software[51], Igor Pro 7.0 (Wavemetrics, Portland, USA) and Statistica 13.5.0.17 (Statsoft, Tulsa, USA). The CETESB is charged with measuring and establishing policies to improve air quality in the state of São Paulo. The CETESB network of air quality monitoring stations is densest in the MASP, and there is therefore no data for some small urban areas. Concentrations measured in the mobile laboratory were compared and analysed in relation to those in the CETESB database.

The initial analysis consisted of an overview of air quality and meteorological variables. The quantile regression model was applied to assess the relationship between the response variable (O_3 concentration quantile) and the explanatory variables (CO, NO, NO_2, wind speed, solar radiation and temperature). The model can provide information about linear and nonlinear relationships between variables[25,52–54].

To discriminate the effect of regional transport on O_3 concentrations throughout the day, we applied polar annulus plots, CPF plots and bivariate polar plots[33]. We estimated the contribution of regional transport to the local O_3 concentration from the parameters of the linear regression analysis between O_x and NO_x[55]. Considering that NO, NO_2 and O_3 are in photostationary states during the daylight hours, we calculated the mean concentration (in ppbv) for the 6:00 a.m.–6:00 p.m. LT. In the equation, the intercept (i.e. the NO_x-independent contribution) gives the O_3 contribution to regional transport and the slope (i.e. the NO_x-dependent contribution) gives the contribution of primary pollutants.

DATA AVAILABILITY

Air quality data from Botucatu that support the findings of this study are available from the corresponding author upon reasonable request. Air quality data from CETESB air quality monitoring network can be obtained through CETESB/QUALAR website under subscription (https://qualar.cetesb.sp.gov.br/qualar/conDadosHorariosPorParametro.do?method=gerarRelatorio).

CODE AVAILABILITY

Most of the codes used in this work are available in the "openair" manual, which can be accessed at https://davidcarslaw.com/files/openairmanual.pdf. The Mann–Whitney test was made with the software Statistica 13.5.0.17.

Received: 18 October 2020; Accepted: 8 February 2021;
Published online: 17 March 2021

REFERENCES

1. Al-Kindi, S. G., Brook, R. D., Biswal, S. & Rajagopalan, S. Environmental determinants of cardiovascular disease: lessons learned from air pollution. *Nat. Rev. Cardiol.* **17**, 656–672 (2020).
2. Oudin, A. et al. Traffic-related air pollution and dementia incidence in Northern Sweden: a longitudinal study. *Environ. Health Perspect.* **124**, 306–312 (2016).

3. Sampedro, J. et al. Future impacts of ozone driven damages on agricultural systems. *Atmos. Environ.* **231**, 117538 (2020).
4. Tai, A. P. K., Martin, M. V. & Heald, C. L. Threat to future global food security from climate change and ozone air pollution. *Nat. Clim. Change* **4**, 817–821 (2014).
5. Ren, W. et al. Impacts of tropospheric ozone and climate change on net primary productivity and net carbon exchange of China's forest ecosystems. *Glob. Ecol. Biogeogr.* **20**, 391–406 (2011).
6. Vandyck, T. et al. Air quality co-benefits for human health and agriculture counterbalance costs to meet Paris Agreement pledges. *Nat. Commun.* **9**, 4939 (2018).
7. Kumar, P. et al. The nexus between air pollution, green infrastructure and human health. *Environ. Int.* **133**, 105181 (2019).
8. Lelieveld, J. et al. Effects of fossil fuel and total anthropogenic emission removal on public health and climate. *Proc. Natl Acad. Sci. USA* **116**, 7192–7197 (2019).
9. Cook, R. et al. Air quality impacts of increased use of ethanol under the United States' Energy Independence and Security Act. *Atmos. Environ.* **45**, 7714–7724 (2011).
10. Union of the Sugarcane Industry. *Consumo de combustíveis* (UNICA, 2020). http://unicadata.com.br/historico-de-consumo-de-combustiveis.php?idMn=11&tipoHistorico=10&acao=visualizar&idTabela=2456&produto=Etanol%2Bhidratado%2Bcombust%2526iacute%253Bvel&nivelAgregacao=1.
11. Renewable Fuels Association. *Annual World Fuel Ethanol Production (Mil. Gal.)* (RFA, 2020). https://ethanolrfa.org/statistics/annual-ethanol-production/.
12. Brazilian Institute of Geography and Statistics - IBGE. Área plantada, área colhida, quantidade produzida, rendimento médio e valor da produção das lavouras temporárias (2018). https://sidra.ibge.gov.br/Tabela/1612.
13. Urban, R. C., Alves, C. A., Allen, A. G., Cardoso, A. A. & Campos, M. L. A. M. Organic aerosols in a Brazilian agro-industrial area: speciation and impact of biomass burning. *Atmos. Res.* **169**, 271–279 (2016).
14. Kawashima, A. B. et al. Estimates and spatial distribution of emissions from sugar cane bagasse fired thermal power plants in Brazil. *J. Geosci. Environ. Protect.* **3**, 72–76 (2015).
15. Kawashima, A. B. et al. Development of a spatialized atmospheric emission inventory for the main industrial sources in Brazil. *Environ. Sci. Pollut. Res.* **27**, 35941–35951 (2020).
16. Young, P. J. et al. Pre-industrial to end 21st century projections of tropospheric ozone from the Atmospheric Chemistry and Climate Model Intercomparison Project (ACCMIP). *Atmos. Chem. Phys.* **13**, 2063–2090 (2013).
17. United Nations Environment. *Integrated Assessment of Short-Lived Climate Pollutants in Latin America and the Caribbean* (UNEP, 2018).
18. United Nations. *The World's Cities in 2018. The World's Cities in 2018—Data Booklet (ST/ESA/ SER.A/417)* (UN, 2019).
19. Alvim, D. S. et al. Main ozone-forming VOCs in the city of Sao Paulo: observations, modelling and impacts. *Air Qual. Atmos. Health* **10**, 421–435 (2017).
20. Andrade, M. F. et al. Air quality in the megacity of São Paulo: evolution over the last 30 years and future perspectives. *Atmos. Environ.* **159**, 66–82 (2017).
21. Carvalho, V. S. B. et al. Air quality status and trends over the metropolitan area of São Paulo, Brazil as a result of emission control policies. *Environ. Sci. Policy* **47**, 68–79 (2015).
22. Chiquetto, J. B. et al. Air quality standards and extreme ozone events in the São Paulo megacity. *Sustainability* **11**, 3725 (2019).
23. Martins, L. D. et al. The role of medium-sized cities for global tropospheric ozone levels. *Energy Procedia* **95**, 265–271 (2016).
24. Salvo, A. & Wang, Y. Ethanol-blended gasoline policy and ozone pollution in São Paulo. *J. Assoc. Environ. Resour. Econ.* **4**, 731–794 (2017).
25. Schuch, D. et al. A two decades study on ozone variability and trend over the main urban areas of the São Paulo state, Brazil. *Environ. Sci. Pollut. Res. Int.* **26**, 31699–31716 (2019).
26. Targino, A. C. et al. Surface ozone climatology of South Eastern Brazil and the impact of biomass burning events. *J. Environ. Manag.* **252**, 1–12 (2019).
27. Doherty, R. M. Ozone pollution from near and far. *Nat. Geosci.* **8**, 664–665 (2015).
28. Lin, M., Horowitz, L. W., Oltmans, S. J., Fiore, A. M. & Fan, S. Tropospheric ozone trends at Mauna Loa Observatory tied to decadal climate variability. *Nat. Geosci.* **7**, 136–143 (2014).
29. Madronich, S. et al. Changes in air quality and tropospheric composition due to depletion of stratospheric ozone and interactions with changing climate: Implications for human and environmental health. *Photochem. Photobiol. Sci.* **14**, 149–169 (2015).
30. Boian, C. & Andrade, M. F. Characterization of ozone transport among metropolitan regions. *Rev. Bras. Meteorol.* **27**, 229–242 (2012).
31. Secretaria de Infraestrutura e Meio Ambiente - SIMA. Balanço Energético do Estado de São Paulo Ano-Base: 2018. 279 pp (2019). Available at https://smastr16.blob.core.windows.net/home/2019/09/corr_beesp2019ab2018bx.pdf.
32. Brazilian National Environmental Council Resolution. *Resolução n. 491, 19 de Novembro de 2018* (CONAMA, 2018). http://www2.mma.gov.br/port/conama/legiabre.cfm?codlegi=740.
33. Carslaw, D. C. The openair manual—open-source tools for analysing air pollution data. Manual for version 2.6-6, University of York. 224 pp (2019). Available at https://davidcarslaw.com/files/openairmanual.pdf.
34. Monks, P. S. et al. Tropospheric ozone and its precursors from the urban to the global scale from air quality to short-lived climate forcer. *Atmos. Chem. Phys.* **15**, 8889–8973 (2015).
35. Finlayson-Pitts, B. J. & Pitts, J. N. Atmospheric chemistry of tropospheric ozone formation: scientific and regulatory implications. *Air Waste* **43**, 1091–1100 (1993).
36. Petroleum, Natural Gas, and Biofuels National Agency - ANP. Anuário Estatístico (2020). http://www.anp.gov.br.
37. Suarez-Bertoa, R. et al. Primary emissions and secondary organic aerosol formation from the exhaust of a flex-fuel (ethanol) vehicle. *Atmos. Environ.* **117**, 200–211 (2015).
38. Corrêa, S. M. et al. Five years of formaldehyde and acetaldehyde monitoring in the Rio de Janeiro downtown area - Brazil. *Atmos. Environ.* **44**, 2302–2308 (2010).
39. Alvim, D. S. et al. Determining VOCs reactivity for ozone forming potential in the megacity of São Paulo. *Aerosol Air Qual. Res.* **18**, 2460–2474 (2018).
40. Nogueira, T., Dominutti, P. A., Fornaro, A. & Andrade, M. F. Seasonal trends of formaldehyde and acetaldehyde in the megacity of São Paulo. *Atmosphere* **8**, 144 (2017).
41. Dominutti, P. A., Nogueira, T., Fornaro, A. & Borbon, A. One decade of VOCs measurements in São Paulo megacity: composition, variability, and emission evaluation in a biofuel usage context. *Sci. Total Environ.* **738**, 139790 (2020).
42. Carter, W. P. L. *Updated Maximum Incremental Reactivity Scale and Hydrocarbon Bin Reactivities for Regulatory Applications*. California Air Resources Board, CA, USA (2010). https://ww3.arb.ca.gov/regact/2009/mir2009/mir10.pdf.
43. Silva Júnior, R. S., Oliveira, M. G. L. & Andrade, M. F. Weekend/weekday differences in concentrations of ozone, nox, and non-methane hydrocarbon in the metropolitan area of São Paulo. *Rev. Bras. Meteorol.* **24**, 100–110 (2009).
44. Wang, Y. et al. CO2 and its correlation with CO at a rural site near Beijing: Implications for combustion efficiency in China. *Atmos. Chem. Phys.* **10**, 8881–8897 (2010).
45. Pollack, I. B. et al. Airborne and ground-based observations of a weekend effect in ozone, precursors, and oxidation products in the California South Coast Air Basin. *J. Geophys. Res. Atmos.* **117**, D00V05 (2012).
46. Gamage, L. P., Hix, E. G. & Gichuhi, W. K. Ground-based atmospheric measurements of CO:CO2 ratios in Eastern Highland Rim using a CO tracer technique. *ACS Earth Space Chem.* **4**, 558–571 (2020).
47. Chandra, N., Lal, S., Venkataramani, S., Patra, P. K. & Sheel, V. Temporal variations of atmospheric CO2 and CO at Ahmedabad in western India. *Atmos. Chem. Phys.* **16**, 6153–6173 (2016).
48. Francisco, A. P., Alvim, D. S., Gatti, L. V., Pesquero, C. R. & De Assunção, J. V. Ozônio Troposférico e Compostos Orgânicos Voláteis em Região Impactada pela Agroindústria Canavieira. *Quim. Nova* **39**, 1177–1183 (2016).
49. Environmental Protection Agency. *Qualidade do ar no estado de São Paulo—2018* (CETESB, 2019). http://ar.cetesb.sp.gov.br/publicacoes-relatorios/.
50. Brazilian Institute of Geography and Statistics - IBGE. Cidades e Estados (2020). https://www.ibge.gov.br/cidades-e-estados/sp/botucatu.html.
51. R. *The R Project for Statistical Computing* (R, 2020). https://www.r-project.org/.
52. Baur, D., Saisana, M. & Schulze, N. Modelling the effects of meteorological variables on ozone concentration—a quantile regression approach. *Atmos. Environ.* **38**, 4689–4699 (2004).
53. Munir, S., Chen, H. & Ropkins, K. An investigation into the association of ozone with traffic-related air pollutants using a quantile regression approach. *WIT Trans. Biomed. Health* **15**, 21–32 (2011).
54. Sousa, S. I. V., Pires, J. C. M., Martins, F. G., Pereira, M. C. & Alvim-Ferraz, M. C. M. Potentialities of quantile regression to predict ozone concentrations. *Environmetrics* **20**, 147–158 (2009).
55. Clapp, L. J. & Jenkin, M. E. Analysis of the relationship between ambient levels of O3, NO2 and NO as a function of NOx in the UK. *Atmos. Environ.* **35**, 6391–6405 (2001).
56. MAPBIOMAS. Mapeamento Anual da Cobertura e Uso do Solo do Brasil (2020). https://mapbiomas.org/.

ACKNOWLEDGEMENTS

The authors would like to thank the Fundação de Amparo à Pesquisa do Estado de São Paulo (FAPESP, São Paulo Research Foundation; Grants nos 16/18438-0 and 2017/17047-0), Petrobras (Grant no. 5850.0103415.17.9) and the Brazilian Conselho Nacional de Desenvolvimento Científico e Tecnológico (CNPq, National Council for Scientific and Technological Development; Grants no. 306862/2018-2 and no. 309514/2019-3) for providing financial support. The authors are also grateful to the

School of Agronomic Sciences of the Universidade Estadual Paulista (UNESP, São Paulo State University) at Botucatu (Lageado Campus), which provided all of the necessary support during the campaigns, and to the CETESB (www.cetesb.sp.gov.br), for providing access to the relevant data.

AUTHOR CONTRIBUTIONS

E.D.F. designed the research project. R.S., T.N., R.A., E.D.F. and M.F.A. conducted the experiments. R.S. and T.N. performed the data analysis. E.D.F., L.D.M., J.M., M.F.A. and C.B.M. contributed to interpretation of the data and preparation of the manuscript. R. S. and T.N. wrote the manuscript with contributions from all authors.

COMPETING INTERESTS

The authors declare no competing interests.

ADDITIONAL INFORMATION

Supplementary information The online version contains supplementary material available at https://doi.org/10.1038/s41612-021-00173-y.

Correspondence and requests for materials should be addressed to R.S. or E.D.d.F.